Spin-Seebeck Effect: A Phonon Driven Spin Distribution

C. M. Jaworski, J. Yang, S. Mack, D. D. Awschalom, R. C. Myers, and J. P. Heremans

Phys. Rev. Lett. **106**, 186601 — Published 2 May 2011

DOI: 10.1103/PhysRevLett.106.186601

The spin-Seebeck effect: a phonon driven spin distribution

C. M. Jaworski[1], J. Yang[2], S. Mack[3], D. D. Awschalom[3], R. C. Myers[2,4*], and J. P. Heremans[1,4*]

1. Department of Mechanical Engineering, The Ohio State University, Columbus, OH
2. Department of Materials Science and Engineering, The Ohio State University, Columbus, OH
3. Center for Spintronics and Quantum Computation, University of California, Santa Barbara, CA
4. Department of Physics, The Ohio State University, Columbus, OH

*To whom correspondence should be addressed. Email: heremans.1@osu.edu, myers.1079@osu.edu

Here we report on measurements of the spin-Seebeck effect of GaMnAs over an extended temperature range alongside the thermal conductivity, specific heat, magnetization, and thermoelectric power. The amplitude of the spin-Seebeck effect in GaMnAs scales with the thermal conductivity of the GaAs substrate and the phonon-drag contribution to the thermoelectric power of the GaMnAs, demonstrating that phonons drive the spin redistribution. A phenomenological model involving phonon-magnon drag explains the spatial and temperature dependence of the measured spin distribution.

PACS numbers: 72.20.Pa, 75.50.Pp, 73.50.Jt, 85.75.-d

The spin-Seebeck effect, consisting of a thermally generated spin redistribution, has been observed in spin-polarized metals[1], semiconductors[2] and insulators[3, 4, 5]. While the experimental evidence has been reproduced by several groups, recent theoretical developments[6, 7, 8] have not been able to explain simultaneously the combination of the persistence of the effect after the severance of electrical communication, the positional dependence, and the temperature dependence[1, 2, 3]. Here we provide a detailed

characterization of the temperature dependence of the spin-Seebeck coefficient (S_{xy}), magnetization (M), and thermoelectric power (thermopower or α_{xx}) of the ferromagnet (FM), alongside the thermal conductivity (κ) and specific heat (C_p) of the substrate. These measurements reveal a direct correlation with the amplitude and temperature dependence of the S_{xy} in multiple samples from which we conclude that the spin-Seebeck effect is driven by phonons. A simple phenomenological model involving phonon-magnon drag (PMD) explains the general features of the temperature and spatial dependence of the spin-Seebeck effect in GaMnAs.

The spin-Seebeck effect produces a voltage across a platinum strip deposited on top of a FM (with a sub-nm Ti adhesion layer in between) in response to an applied temperature gradient. The sample geometry is shown in Fig 1 and is the same as Refs. [1, 2, 3, 9]. Unlike classical transport coefficients, S_{xy} is not uniform across a sample, but depends spatially on the position x around the center of the sample, following a $S_{xy} \propto \sinh(x/\lambda - b)$ relation with a characteristic length scale λ of millimeters, which persists without electrical communication between ends of the sample. One end of the sample is heated (x= -L/2), the other cooled (x= +L/2), thus creating a longitudinal gradient ∇T_x. The electric field developed by the Pt strips along the *y* direction by spin-polarization in GaMnAs is measured. A spin-current traveling (along *z*) from the FM into the Pt is scattered by the inverse spin Hall effect (ISHE) and generates the electric field E_{ISHE} [10]. We measure E_{ISHE} as a voltage V_y across the Pt strips and sweep magnetic field (along x) in a hysteretic manner to realize reversals in direction of E_{ISHE} at the coercive field as a measurable ΔV_y. We subsequently subtract out residual voltages and EMF pickup from sweeping magnetic field, thus centering the V_y signal around zero volts. The linearity of ΔV_y vs. ΔT_x has been shown elsewhere[2], and enables us to define S_{xy} as half of

ΔV_y normalized by width of sample (w) and distance between the thermometry (L), $S_{xy} \equiv \frac{E_y}{\nabla_x T} = \frac{L\Delta V_y}{2w\Delta T_x}$. The positional dependence of $S_{xy}(x) \propto \sinh(x/\lambda - b)$ has been shown in Ref. [2]; here we concentrate on the magnitude S_{xy} on a contact near x=-L/2, where it is maximal. Given the definitions above, $S_{xy}(-L/2)<0$, and $S_{xy}(+L/2)>0$, and preliminary data on other ferromagnets[2, 11] show that these signs are material-dependent. The experimental methods and sample preparation are the same as in Ref. [2] but in a modified cryostat (TTO in a Quantum Design PPMS) that enables a better heat sinking. We measure κ and α_{xx} using a classic heater-and-sink method, C_p using a quasi-adiabatic platform calorimeter, and M with a SQUID magnetometer. Data were measured on 10 nm thick Pt strips with 1 nm of Ti for adhesion on two samples 4×12 mm^2 of 30 nm thick $Ga_{0.842}Mn_{0.158}As$ (Fig. 2) or 5×15.5 mm^2 100 nm thick $Ga_{0.84}Mn_{0.16}As$ (Fig. 3) with a magnetic easy axis along $[\bar{1}10]$ grown on 0.5 mm thick semi-insulating GaAs by molecular beam epitaxy[2, 12]. The error in S_{xy} is estimated by dividing the RMS of the noise on the voltmeter (Keithley 2182A) by ΔT_x whereas other error estimates are provided by the instrumentation software.

In Fig. 2 we show $S_{xy}(T)$, M, and α_{xx} of one GaMnAs sample (green stars) alongside κ of the sample substrate. C_p is given in the inset to Fig. 2a, and portions of S_{xy} and κ data are fitted to power laws. α_{xx} of another piece of the similar sample (purple circles) extended to lower temperature (Fig. 2c) illustrates the phonon-drag effect on α_{xx}. κ and C_p are actually the sum of the contributions of both the GaAs substrate and the 30nm thick GaMnAs film, but the phonons in the 0.5 mm thick substrate dominate. M shows a ferromagnetic behavior with $T_c \sim$ 135 K. We note four distinct temperature regimes, separated by vertical dashed lines, in the spin-Seebeck effect in Fig. 2.

(1) Above the Curie temperature (T_c) of 135 K the sample is a paramagnet, and $S_{xy} \sim 0$.

(2) Between 135-85 K both M and S_{xy} show an order parameter behavior $(T_c-T)^{-\gamma}$. S_{xy} increases in magnitude with decreasing T to $|S_{xy}| \sim 0.25$ μV/K, demonstrating the dependence on M. κ increases with decreasing T but more slowly than either M or S_{xy}. α_{xx} is proportional to T as expected in a degenerately-doped semiconductor.

(3) Between 85-35 K, M varies more slowly with T. κ increases with decreasing T as a T^{-1} law, characteristic of phonon-phonon Umklapp scattering, then reaches a maximum at 35 K. S_{xy} follows κ closely up to a peak of ~1.05 μV/K at 35 K and both S_{xy} and κ peak at the same T. α_{xx} departs from the T^1 and the difference forms a peak also slightly below 35 K indicative of phonon-electron drag (PED).

(4) Below 35 K, there is a sharp decrease in S_{xy} with decreasing T following a $T^{3/2}$ law, with $|S_{xy}|$ reaching ~0.4 μV/K at 15 K. This $T^{3/2}$ behavior is reminiscent of the T-dependence of a magnon specific heat[13]. C_p of the substrate follows a T^3 law consistent with the Debye model, with a slight excess in C_p appearing at higher T. κ also follows a T^3 law down to 10 K: this is understood by realizing that the phonon mean free path Λ now is a constant, and $\kappa = 1/3\ C_p\ v\ \Lambda$, where v is the sound velocity. The PED effect on α_{xx} decreases at lower T where it diminishes to zero at 0 K.

The above trends are reproduced on a second sample grown on a higher quality GaAs substrate with ten times higher peak κ (Fig. 3). The maximum in κ(T) is now lowered to ~10-15 K. S_{xy} now peaks at 10 K instead of 35 K in the previous sample (Fig. 2). As the two different processed samples are not identical, we refrain from a direct comparison. We note that the sample in Fig. 2 at 50 K has $|S_{xy}|$ ~0.75 μV/K which peaks at ~1.05 μV/K at 35 K, while the sample in Fig. 3 at 50 K $|S_{xy}|$ ~0.2 μV/K which peaks at ~ 4 μV/K at 10 K. The magnitude

scales roughly with κ. The PED peak in α_{xx} is now prominent with a maximum again at ~10-15 K. This reveals that S_{xy} scales with κ of the substrate as well as with the intensity of PED in α_{xx} as a function both of substrate condition and of T.

The observation that S_{xy} scales with κ and phonon-electron drag (PED) is consistent with recent publications invoking phonon-magnon drag (PMD) as a mechanism at least contributing to S_{xy} in the ferromagnetic insulator YIG[6, 7, 8], although equation (3) in Ref. [8] does not fit our S_{xy} data. First, we review the mechanism behind the PED contribution to α_{xx}. At higher T, the classical diffusion thermopower (α_{xx}) is governed by the Boltzmann equation. In this regime, and for degenerately-doped semiconductors, $\alpha_{xx} \propto T$ as observed above 90 K (Fig. 2c). Here electrons and phonons are constantly being brought back to mutual equilibrium by collisions, and the ∇T only slightly perturbs the electron distribution. When electron-phonon interactions dominate, the PED-α_{xx} adds to the diffusion α_{xx} in the form of a peak at some T. When enough phonons interact with electrons, rather than with other phonons or impurities and defects, they impart momentum to the electrons along ∇T and move the electron distribution away from equilibrium, resulting in an extra PED-α_{xx} that can be orders of magnitude larger than the diffusion-α_{xx} . The amplitude of this effect scales with the ratio between phonon/electron and phonon/phonon or phonon/defects interaction cross-sections, as well as with the density of phonons available to interact with the electrons. Therefore, in metals the PED-α_{xx} peaks at $T=T_{max}$ close to the maximum lattice thermal conductivity. Above T_{max}, Umklapp processes compete with phonon-electron interactions to bring the phonons back to equilibrium, while below T_{max} the number of phonons decreases following the Debye specific heat. The situation in degenerately-doped semiconductors is only slightly different: as observed in Figs. 2 and 3 the T_{max} of the PED contribution can differ somewhat from that of the maximum in κ because it

depends on the size of the Fermi surface and the number of phonons that can interact with electrons on that surface. Comparing Figs. 2 and 3 illustrates that the lower the phonon-phonon and phonon-defect interactions, the higher the relative magnitude of the PED-α_{xx}.

Generalizing these concepts now to PMD, we offer in Fig. 1 a qualitative outline of the role of substrate phonons in the thermally-induced spin distribution. At least in the case of ferromagnetic insulators[6] (comments on the applicability of this to GaMnAs are given below), the driving force for PMD is the difference between the temperature of the magnons $T_M(x)$ in the ferromagnetic film and that of the phonons $T_P(x)$ in the substrate and in the film (Fig. 1a); given the similarities between our observation of the spin-Seebeck effect in GaMnAs and that in YIG[3], we assume a similar case to hold here. In the absence of a gradient, $T_M(x) = T_P(x)$ at all x. The drag force only arises in the presence of a ∇T, which imparts an excess momentum to the phonons: $T_P(x)$ now follows a linear profile between the hot and the cold end of the sample (Fig. 1a). We assume that the temperature baths at the ends of the sample only connect to the phonons, and that the magnons interact with phonons resulting in a $T_M(x)$ profile shown in Fig. 1a. The difference $\Delta T_M(x) = T_P(x) - T_M(x)$ is calculated to follow a $\sinh(x/\lambda)$[13] law (Fig. 1b), and mirrors the observed spatial dependence of S_{xy} [2]. Near the center of the sample, $\Delta T_M(x\sim0)=0$; exactly where this happens depends on the coupling to the reservoirs at the ends of the sample, and can be slightly offset from x = 0. At the hot end of the sample, $\Delta T_M(x < 0) > 0$, PMD tends to heat up the magnons; the reverse holds at the cold end, where phonons cool the magnons, $\Delta T_M(x > 0) < 0$.

Magnons in GaMnAs are perturbations of the ferromagnetic spins residing around Mn ions. The moments fill precession cones (Fig. 1), and the average moment $M_x(T, H_x)$ is their projection along *x*. The zeroth order effect of the ∇T on these moments is via the T-dependence

of $M_x(T_M(x))$ as seen in Fig. 2a. At the hot end, phonon drag heats up the magnons above thermal equilibrium, thus decreasing the M_x by a quantity ΔM_x ($x < 0$) < 0 (Fig. 1c). At the cold end of the sample, PMD cools magnons, increasing M_x by $\Delta M_x(x > 0) > 0$. Thus $\Delta M_x(x) \sim \Delta T_M(x) \sim \sinh(x/\lambda)$. The dependence of ΔM_x on substrate κ and on T is a function of the intensity of the PMD. As with PED, ΔM_x will therefore depend on the density of dragging phonons, and on the ratio of phonon/magnon to phonon/phonon and phonon/impurity interaction cross-sections. This is consistent with the observation that $S_{xy}(T) \sim \kappa(T)$ for T above the maximum in κ for both samples (Figs. 2 and 3). At $T < 35$ K in Fig. 2, where S_{xy} and κ have a maximum, the magnon C_p scales with $T^{3/2}$, rather than the T^3 for the phonons, again consistent with the observed slope of $S_{xy}(T < 35K)$ (Fig. 2b). Similar behavior is observed in Fig. 3, where the maximum now appears at a lower T of 15 K.

Last, we consider the effect of $\Delta M_x(x)$ on the distribution of spin-polarized electrons. In GaMnAs, the charge carriers are highly spin-polarized (85%) holes[14]. The fact that a true zero (not an offset) is measured[2] for $S_{xy}(x\sim0)$ indicates that spin polarized holes are not simply thermally diffusing into Pt since otherwise we would measure a signal even near $x = 0$ due to the inherent spin polarization of GaMnAs. Perhaps the non-equilibrium spin distribution (Fig. 1) is maintained by a continuous transfer of angular momentum to magnons requiring, by conservation, a flow of angular momentum in the form of a balancing spin-current that generates a voltage due to ISHE either in the Pt transducers or in the GaMnAs layer itself (Fig. 5 of Ref. [2]). This behavior would be consistent with the model proposed in Refs. [6, 15] where the thermal perturbation of magnons leads to spin pumping in the Pt layers.

Reverting to the applicability of the model of Refs. [6, 13] to GaMnAs, where the spin diffusion length is many orders of magnitude shorter than in YIG, one can point out that the spin

diffusion length and PMD are related. When the magnon-phonon coupling is weak, as in YIG, $|T_M-T_P|$ is large, but the PMD coupling small. Conversely, in GaMnAs one expects $|T_M-T_P|$ to be much smaller than in YIG, but the coupling to be much stronger, so that S_{xy} in metals, semiconductors and insulators ends up similar to within a few orders of magnitude.

The thermodynamic coupling of spins and phonons opens opportunities for fundamentally new spin-caloric concepts, either in reversible thermodynamics or in transport. This may lead to phonon engineering of spin-based devices, where heat transfer can be integrated with magnetic functionality and may result in fundamentally new applications, like spin-based cooling, or magnetically sensitive thermoelectrics and bolometers.

The authors thank E. Johnston-Halperin and K. J. Wickey for useful discussions. This work was supported in parts by the Center for Emergent Materials at OSU, an NSF MRSEC (Award # DMR-0820414), NSF (including Award # CBET-0754023), the ONR, Ohio Eminent Scholar Discretionary funding, and OSU Institute for Materials Research.

References

[1] K. Uchida *et al.*, Nature **455**, 778 (2008).

[2] C. M. Jaworski *et al.*, Nature Materials **9**, 898 (2010).

[3] K. Uchida *et al.*, Nature Materials **9**, 894 (2010).

[4] K. Uchida *et al.*, Appl. Phys. Lett. **97**, 172505 (2010).

[5] K. Uchida, T. Nonaka, T. Ota, and E. Saitoh, Appl. Phys. Lett. **97**, 262504 (2010).

[6] J. Xiao *et al.*, Phys. Rev. B **81**, 214418 (2010).

[7] H. Adachi, J.-i. Ohe, S. Takahashi, and S. Maekawa, Phys. Rev. B **83**, 094410 (2011).

[8] H. Adachi *et al.*, Appl. Phys. Lett. **97**, 252506 (2010).

[9] K. Uchida *et al.*, Sol. Stat. Comm. **150**, 524 (2010).

[10] E. Saitoh, M. Ueda, H. Miyajima, and G. Tatara, Appl. Phys. Lett. **88**, 182509 (2006).

[11] T. Ota *et al.*, J. Phys.: Conf. Ser. **200**, 062020 (2010).

[12] S. Mack *et al.*, Appl. Phys. Lett. **92**, 192502 (2008).

[13] D. J. Sanders and D. Walton, Phys. Rev. B **15**, 1489 (1977).

[14] J. G. Braden *et al.*, Phys. Rev. Lett. **91**, 056602 (2003).

[15] M. Hatami, G. E. Bauer, S. Takahashi, and S. Maekawa, Sol. Stat. Comm. **150**, 480 (2010).

Figure Captions

FIG. 1 (color). Top schematic shows the experimental setup (not to scale). (a) Temperature profile of phonons and magnons. (b) The temperature difference between phonons and magnons. Cartoon showing the effect of phonon drag on the magnetic moment M_x in each region. (c) Change in M_x due to phonon drag across the temperature gradient. (d) Schematic hysteresis loops representing the transverse voltage detected on the Pt strips in each region.

FIG. 2 (color). Thermal properties of one GaMnAs/GaAs sample versus temperature. (a) M of the GaMnAs and κ of the GaAs substrate. Fit quality: $a+bT^3$: $R^2 = 0.98$, T^{-1} : $R^2 = 0.98$, $T_c\text{-}T^{-\gamma}$: $R^2 = 0.99$. The inset shows the substrate C_p. (b) S_{xy} of the GaMnAs. Fits quality: $a+bT^{1.5}$: $R^2 = 0.95$, $a+bT^{-1}$: $R^2 = 0.92$, $T_c\text{-}T\text{-}^{\gamma}$: $R^2 = 0.95$. (c) α_{xx} of the sample (green stars) and of a similar sample (purple dots).

FIG. 3 (color). Thermal properties of a second GaMnAs sample grown on a substrate with higher κ. (a) S_{xy} and κ, and (b) α_{xx} and M as a function of temperature.

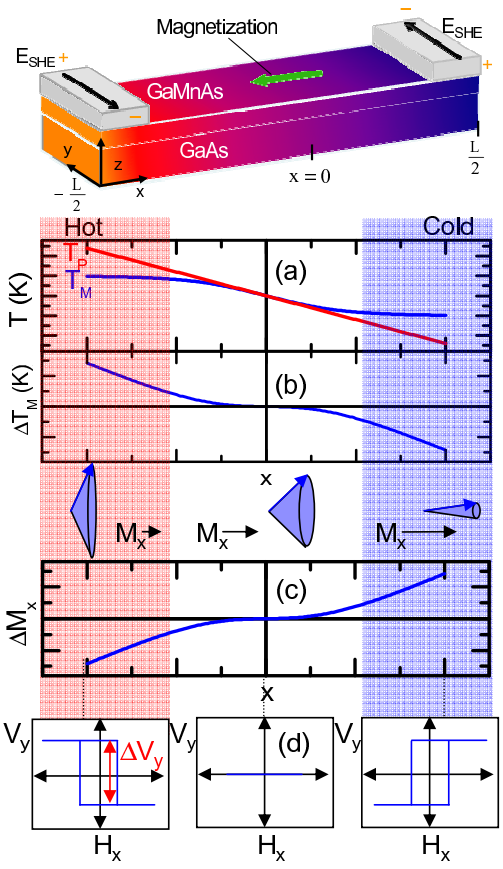

Fig. 1, Jaworski et al.

Figure 1 LB12713 04APR2011

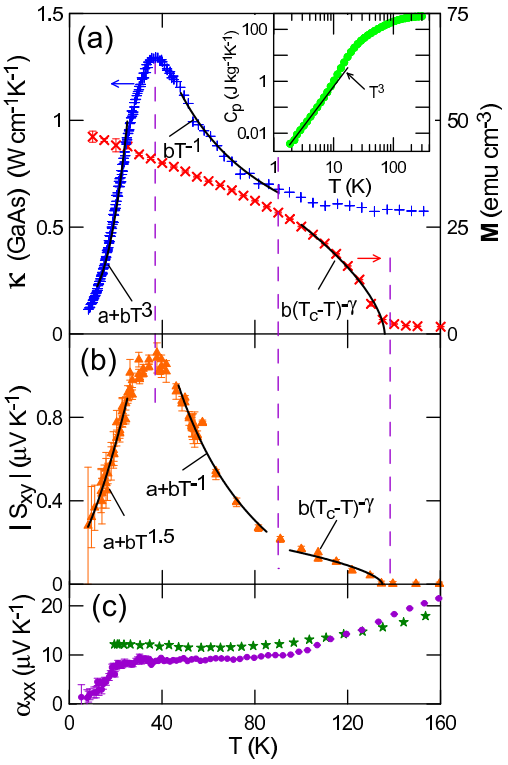

Fig. 2, Jaworski et al.

Figure 2 LB12713 04APR2011

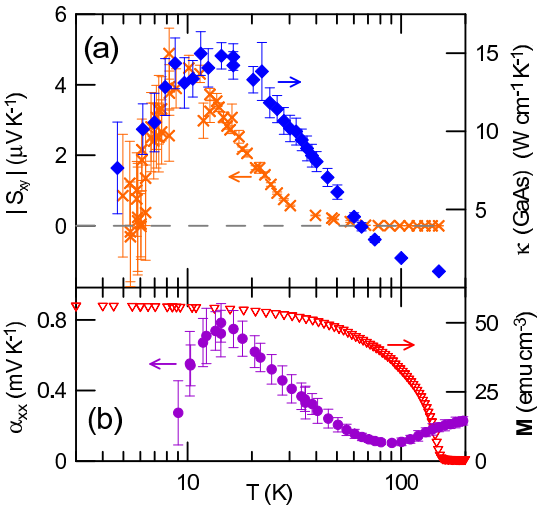

Fig. 3, Jaworski et al.

Figure 3 LB12713 04APR2011